Nuclear Instruments and Methods in Physics Research A 419 (1998) 556–569

NUCLEAR INSTRUMENTS & METHODS IN PHYSICS RESEARCH Section A

Radiation damage of silicon strip detectors in the NA50 experiment

B. Alessandro[a], S. Beolé[a], G. Bonazzola[a], E. Crescio[a], W. Dąbrowski[b], P. Giubellino[a], P. Grybos[b], M. Idzik[b,*], M. Martinetto[a], A. Marzari-Chiesa[a], M. Masera[a], F. Prino[a], L. Ramello[a], P.R. Mendes[a], L. Riccati[a], M. Sitta[a]

[a] *INFN, Torino, Italy*
[b] *Faculty of Physics and Nuclear Techniques, Academy of Mining and Metallurgy, Al. A. Mickiewicza 30, PL-30-059, Krakow, Poland*

Abstract

During operation of the multiplicity detector in the NA50 experiment the single sided AC-coupled p-on-n silicon strip detectors were exposed to charged particle fluences up to 20^{14} eq n/cm^2 and ionising doses up to 20 Mrad, with a very non-uniform radiation spatial distribution. Radiation effects in the detectors observed during the '96 lead ion run as well as results of the post-run measurements are presented in this paper. © 1998 Elsevier Science B.V. All rights reserved.

Keywords: Silicon strip detectors; Noisy channels; Radiation damage

1. Introduction

The multiplicity detector in the NA50 experiment [1] is one of very few detectors working in a real experiment where silicon detectors are exposed to radiation fluences and doses comparable to the ones expected for the LHC inner trackers [2]. A crucial aspect of such a detector is its radiation resistance. We present here the results on the radiation issue obtained during two years of operation of our detector.

NA50 is a fixed target experiment investigating the production of resonances decaying to dimuons produced in high-energy (158 A GeV/c) Pb–Pb interactions at the CERN SPS. The silicon microstrip detectors are used in the NA50 experiment for charged multiplicity measurements and for target recognition. The layout of the NA50 experiment imposed several important constraints on the design of the silicon multiplicity detector. Given the high interaction rate a very short deadtime of the readout electronics (< 50 ns) was implemented. The radial microstrip detectors were designed with a constant segmentation in pseudorapidity ($\Delta\eta = 0.02$) and in the azimuthal angle ($\Delta\phi = 10^0$). A single detector unit is shown in Fig. 1. It consists of 128 AC-coupled p-on-n strips with a pitch ranging from 90 μm at the tip of the detector to 700 μm in the outermost part. In this paper we refer

* Corresponding author.

PII: S0168-9002(98)00868-7

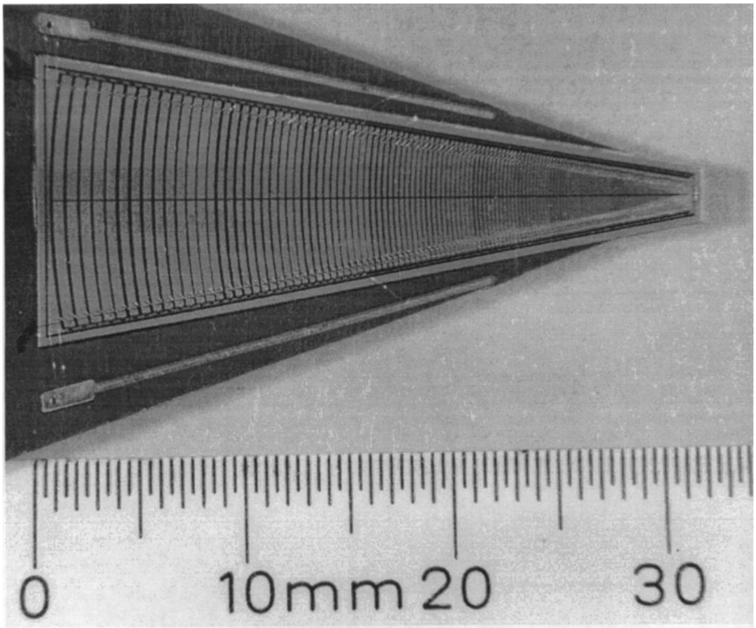

Fig. 1. View of the AC-coupled single detector unit.

to the innermost strip as to the strip number 1 successively numbering the strips up to strip 128, the outermost strip. The design of the detector implies constant occupancy and therefore highly non-uniform radiation levels. Estimated fluences and doses for the innermost part of the detector during the '96 ion run were up to 10^{14} eq n/cm^2 and up to 20 Mrads of ionising radiation, respectively. As a result even the outermost strips, which obtained about 10^{13} eq n/cm^2, were inverted after the '96 ion run.

The paper is divided into two parts. In the first part we discuss the methods to measure radiation damage effects during data taking, together with the results obtained during the '96 ion run. In the second part we present the results of the measurements performed after the run in order to cross-check the on-beam observations and to better understand the behaviour of the detectors after type inversion.

2. Radiation effects observed during the '96 lead run

During the run radiation damage manifested itself mainly with an increase of the leakage currents and of the depletion voltages. The leakage currents were measured directly whereas there was no direct way to measure the depletion voltage during data taking. An observable fact correlated to the depletion voltage change is the occupancy of particles measured in the detector. In the following we will discuss radiation effects observed during the run on the basis of leakage currents and occupancy measured in the detector.

2.1. The leakage current

The leakage currents of the detectors were monitored continuously during the run. In Fig. 2 the leakage currents for detectors irradiated during the '96 run and during both the '95 and '96 ion runs are shown. Some sharp changes of the current are linked to changes in the cooling system, power supply breakdowns, no-beam and bias voltage changes. One can see that in agreement with the phenomenology, currents scale linearily with the received fluence, under the realistic assumption of almost constant average beam intensity. One should notice that the leakage current shown in Fig. 2 is the total current of a detector comprising

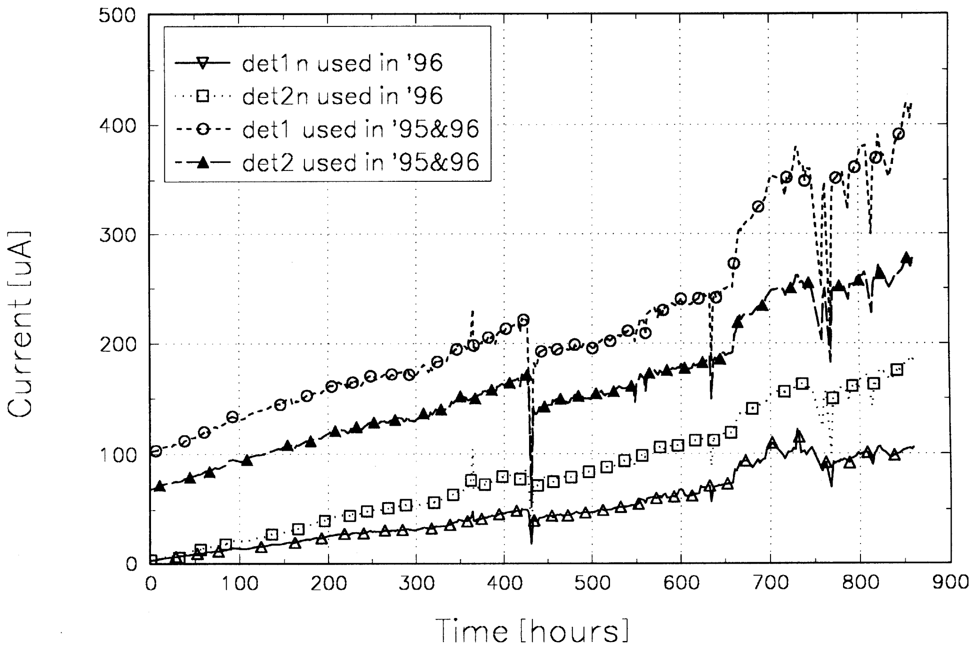

Fig. 2. Typical leakage currents of individual detectors during the '96 ion run.

strips irradiated up to fluences varying by more than one order of magnitude between the innermost and the outermost strips. Therefore the damage constant resulting from these measurements is not comparable to values obtained by other radiation tests, e.g. Ref. [3].

2.2. Breakdown voltage

In the design of the silicon multiplicity detector no special features assuring high voltage operation were employed. Nevertheless, no detector breakdown was observed during the ion run. Fig. 3 shows some of the I–V characteristics measured at the end of the '96 run by varying the detector bias voltage (HV scan). At this stage all detectors were already inverted and no sign of breakdown was visible. In addition, during the post-run measurements bias voltages up to 400 V were applied to many detectors and no breakdown of any detector was observed. All the strips in a single detector were biased with the same voltage although the actual full depletion voltage varied from ~ 20 V, for the outermost strips, to ~ 200 V for the inner ones. All of the 36 non-uniformly irradiated detectors were working successfully after type inversion, with applied bias voltage up to at least 200 V and sometimes 400 V, and none of them became unusable. Our observations confirm the effect of increasing breakdown voltage of p-on-n detectors after type inversion, as observed in other radiation experiments [4].

2.3. Noise during the run

In order to reduce the sensitivity of the system to the detector leakage current and to noise due to this leakage current, AC-coupled strips together with very fast readout electronics ($T_{\mathrm{peak}} = 15$ ns) were implemented. The performance of the system was monitored by means of the number of so-called noisy channels versus time during the run. The definition of a noisy channel was chosen analysing the results of different possible cuts. Finally, the channels with an occupancy higher than 72% or higher than four times the average of the 16

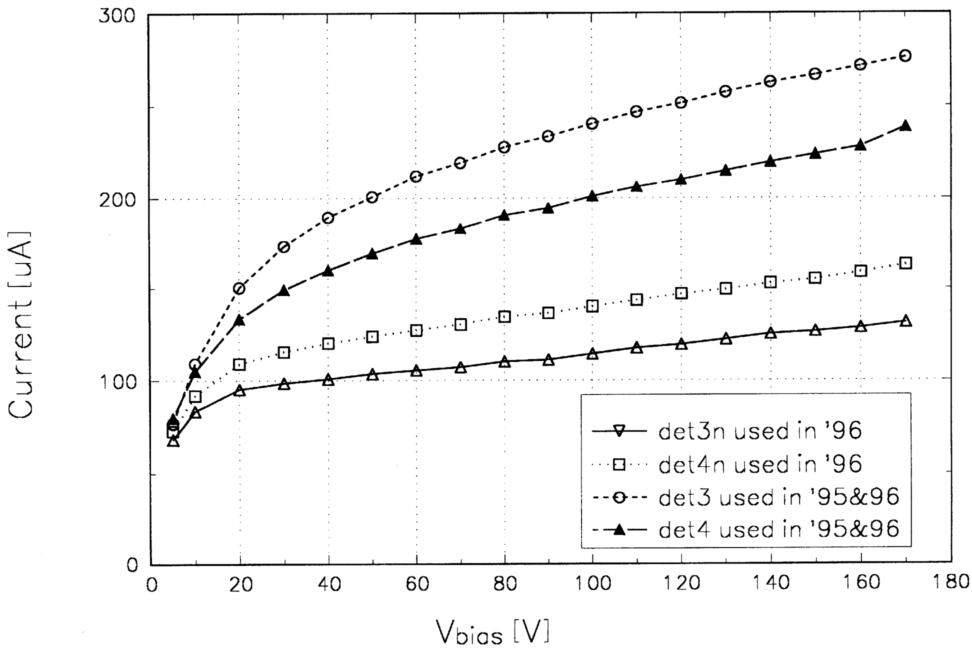

Fig. 3. The leakage currents versus bias voltage at the end of the '96 ion run.

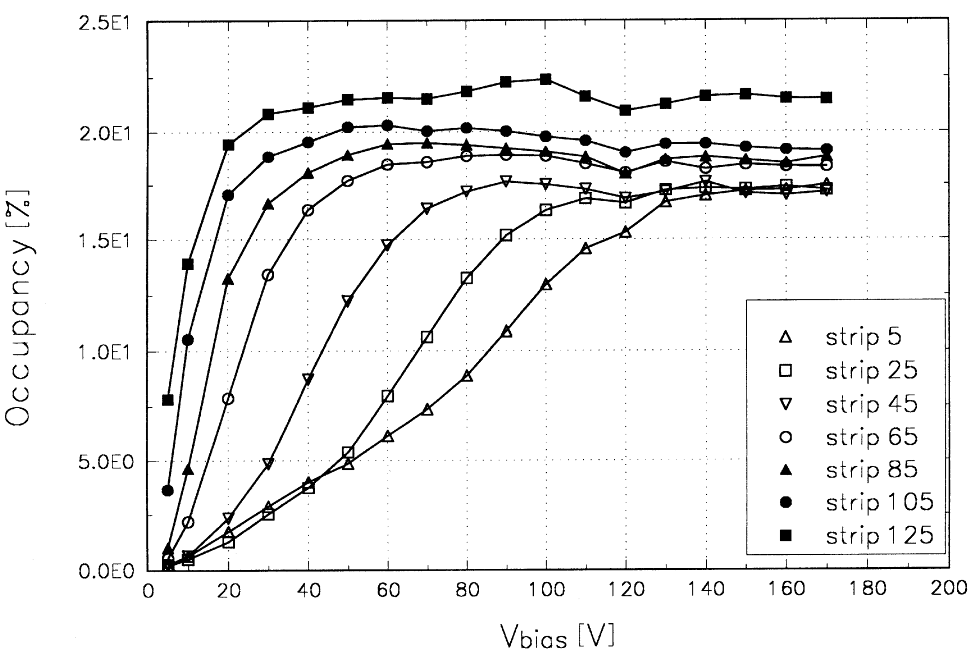

Fig. 4. Strip occupancy versus bias voltage at the end of the '96 ion run for detectors used only in the '96 run.

neighboring strips were classified as noisy. Such a high threshold for the occupancy cut results from the very high (20–30%) physical occupancy of the particles in the detector. No change in the number of noisy channels was observed, which would be correlated to the increase of detector leakage currents.

2.4. Occupancy versus detector bias voltage

At the end of the '96 ion run we performed detector bias voltage scans with the lead beam on in order to measure locally and simultaneously the effects of the irradiation on the detectors. Figs. 4 and 5 show typical curves of the occupancy versus detector bias voltage for detectors used in the '95 as well as in both the '95 and '96 ion runs. One can see that the occupancy for the innermost strips of detectors used in '95 and '96 does not saturate at the highest applied bias voltage. In order to correlate the depletion voltage to the measured occupancy, we assumed in a first approximation that occupancy $\sim Q_{\mathrm{collected}} \sim W_{\mathrm{depleted}} \sim \sqrt{(V_{\mathrm{bias}})}$. Using a simple algorithm, which finds the crossing point of two linear fits, the depletion voltage was evaluated strip by strip (Fig. 6) on the basis of the occupancies obtained during HV scans. It was previously shown [1] that the depletion voltages calculated from the strip occupancy are in good agreement with the ones obtained from C–V measurements. From the data shown in Figs. 5 and 6 it is clear that the depletion voltages of the innermost strips of the detectors used in the '95 and '96 runs exceed the limit of our power supply, which was 200 V during the '96 run. Since these detectors were kept at room temperature between the '95 and the '96 ion runs, one should expect that significant reverse annealing took place [5]. Indeed, although the total fluence in the '95 run was about 1/4 of the '96 run, the depletion voltages for these detectors were more than double of the ones used only in the '96 run. For the '98 ion run the most irradiated detectors will be replaced by new ones.

2.5. Detector efficiency

In order to evaluate the efficiency of irradiated detectors we compared the saturation value of the

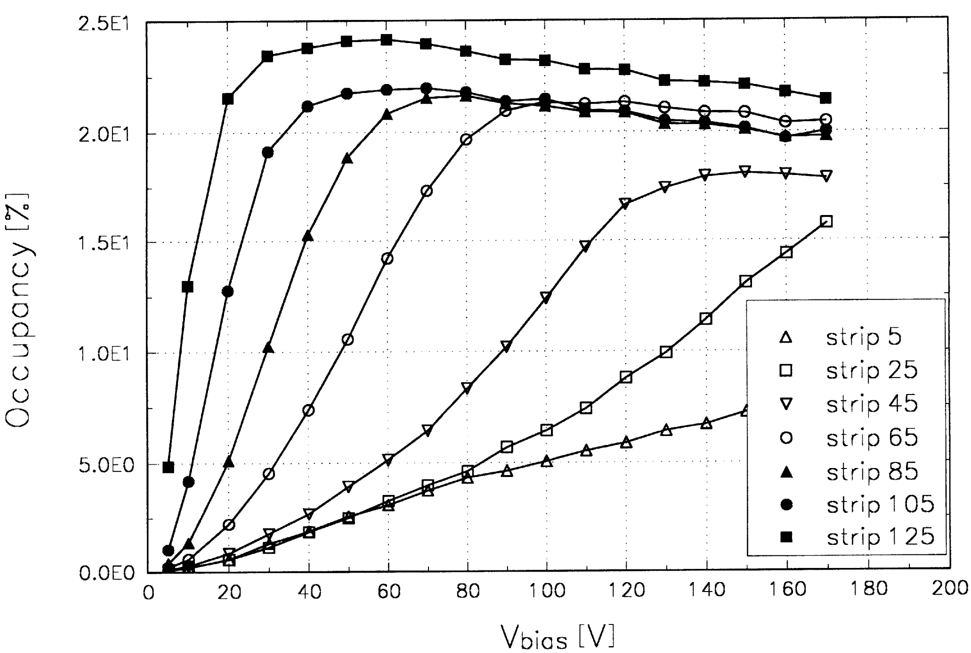

Fig. 5. Strip occupancy versus bias voltage at the end of the '96 ion run for detectors used in both the '95 and the '96 runs.

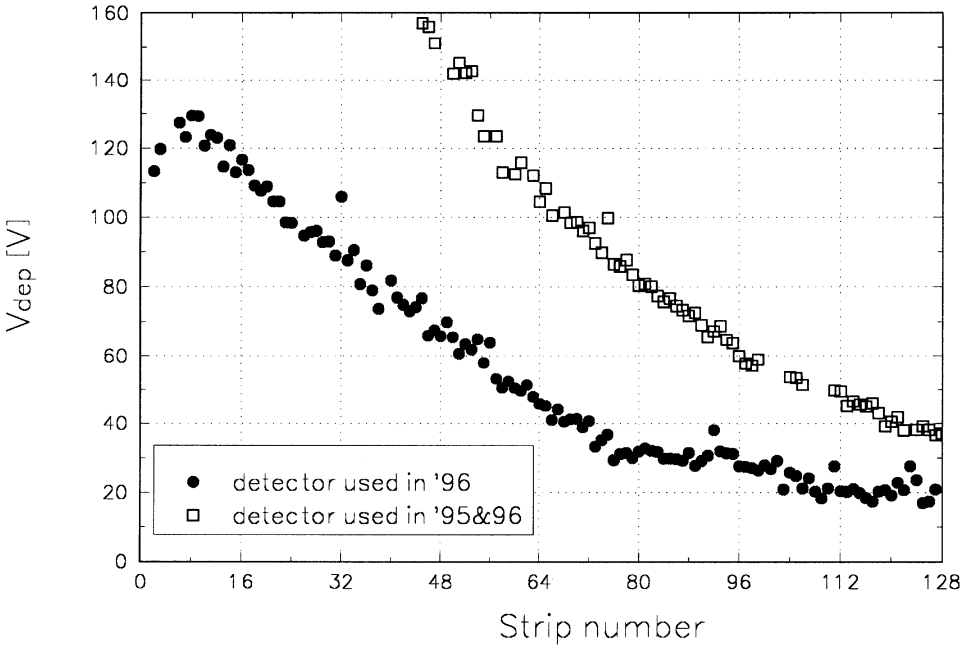

Fig. 6. Strip-by-strip depletion voltages calculated from the occupancies measured in the HV scan.

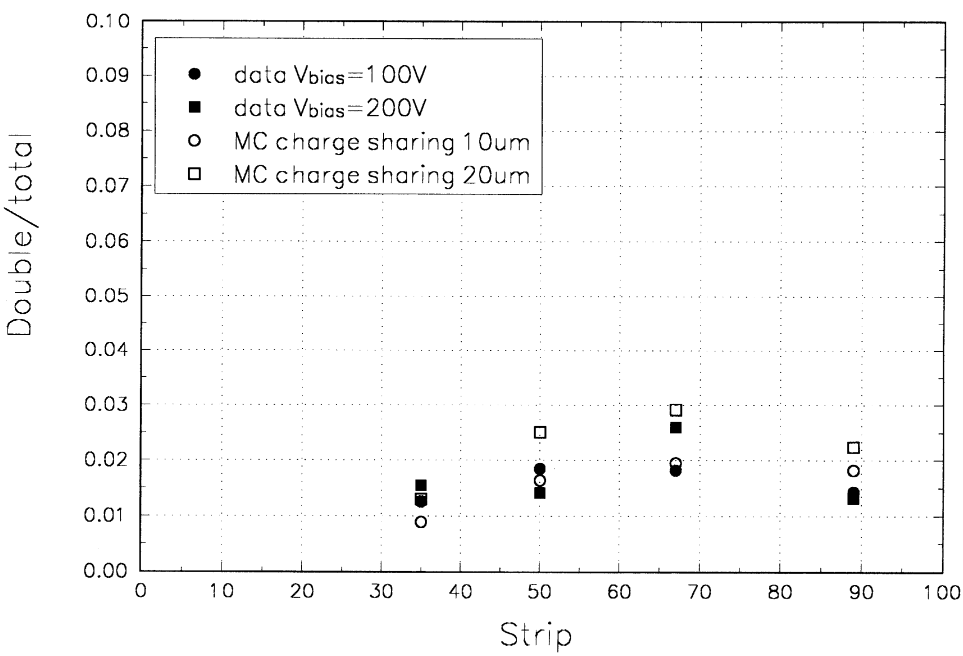

Fig. 7. Ratio of the number of double strip clusters to single strip clusters obtained with a proton-beam and simulated with GEANT.

strip occupancy (shown in Fig. 4) with the physical occupancy of the particles, obtained from the hit-maps at the beginning of the run, when the detectors were not yet irradiated. For strips which were fully depleted, no decrease of the efficiency (with the accuracy of 10%) was observed. Obviously, for strips which were not fully depleted we observed a significant drop of efficiency. We can, however, conclude that standard p-on-n detectors operate successfully at fluences up to 10^{14} eq n/cm^2 and do not show significant loss of efficiency if they are biased at a high enough voltage to be fully depleted.

2.6. Interstrip isolation for the detector after type inversion

After the '96 ion run we performed a beam test exposing the detectors to the primary proton beam in order to investigate the isolation of p + strips after type inversion in the detector. Fig. 7 shows the ratio of double strip clusters to single strip ones, measured for a different bias of the detector (approximately 100 V was enough to deplete the strips above strip number 70 while 200 V depleted the ones above strip number 30). Due to the limited statistics the measured data are affected by an error of about 30%. In Fig. 7 we also show the values simulated with GEANT under the hypothesis of different widths of the charge sharing region in the detector. One can clearly see that in all cases the fraction of double strip clusters is of the order of 2% in good agreement with the Monte Carlo simulation and is not significant in absolute terms. We can conclude that no evidence of lack of isolation between strips of the inverted detector was observed, even for the strips which were not fully depleted.

3. Post-run measurements

In order to cross-check the on-beam observations of radiation effects as well as to investigate in more detail the behaviour of inverted detectors a set of laboratory measurements was performed after the '96 ion run for some of the detectors. We concentrated on standard detector electrical parameters performing AC impedance measurements, using an HP4284A LCR meter, and DC I–V measurements. Keeping in mind that radiation-induced effects are characterized by relatively long time constants, we devoted particular attention to the frequency dependence of the measured quantities. We should note that because of the very non-uniform irradiation each detector unit consists of a sample of strips with depletion voltages ranging from few tenths to a few hundred volts. In the following we present a selection of typical results concerning capacitance to the backplane, interstrip capacitance and AC and DC interstrip resistance. We will also discuss the behaviour of the p + side after type inversion.

3.1. Capacitance to the backplane

Before irradiation the capacitance to the backplane C_{back} was measured and no frequency dependence was observed. This was not the case for the detectors after type inversion. Figs. 8 and 9 shows typical curves of $1/C^2_{\mathrm{back}}$ versus bias voltage for inverted strips, measured in the oscillator frequency range of 10–200 kHz.

One can see that the $1/C^2$ method allows to evaluate the full depletion voltage in this frequency range. Measurements for frequencies below 10 kHz and above 200 kHz were done as well but the shapes of the curves were more complex and did not allow to make simple linear fits. Depletion voltages estimated in this way agree with the ones obtained from the occupancy in the HV scan at the end of the '96 run. Figs. 10 and 11 shows C_{back} versus oscillator frequency, measured for bias voltages below and above the depletion voltage, respectively. The capacitance versus frequency characteristics for the bias voltages below the full depletion voltage show typical shapes indicating the presence of deep energy levels in the band gap [6]. Two dominant radiation induced levels are observed, at ~ 1 kHz and at ~ 50 kHz. After depletion the latter practically disappears. The frequency dependence of C_{back} vanishes for $V_{\mathrm{bias}} \sim 400$ V, which is much higher than $V_{\mathrm{dep}} \sim 40$ V, and C_{back} recovers its purely geometrical value.

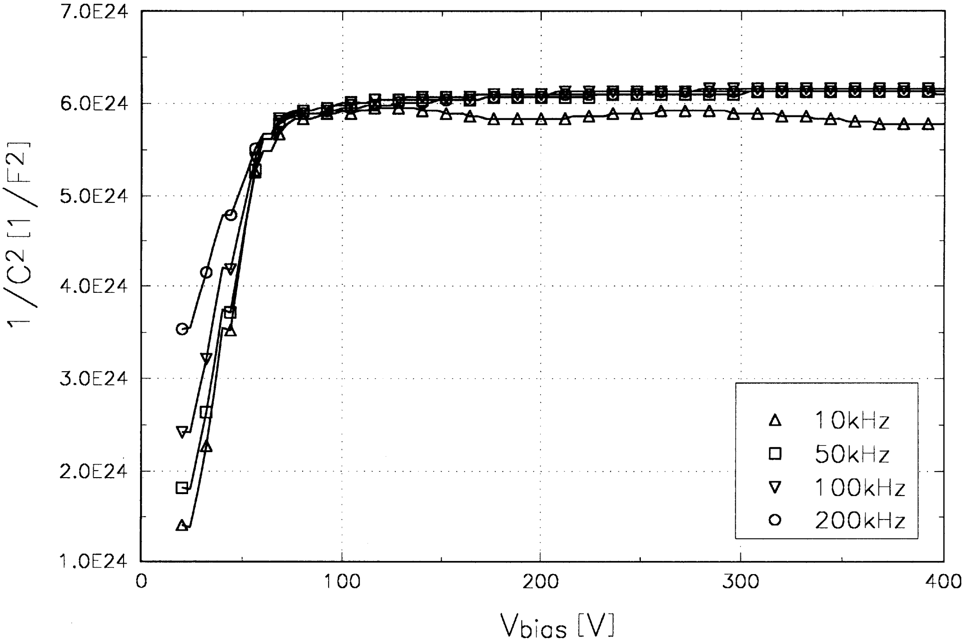

Fig. 8. $1/C^2_{back}$ versus bias voltage for strip number 100.

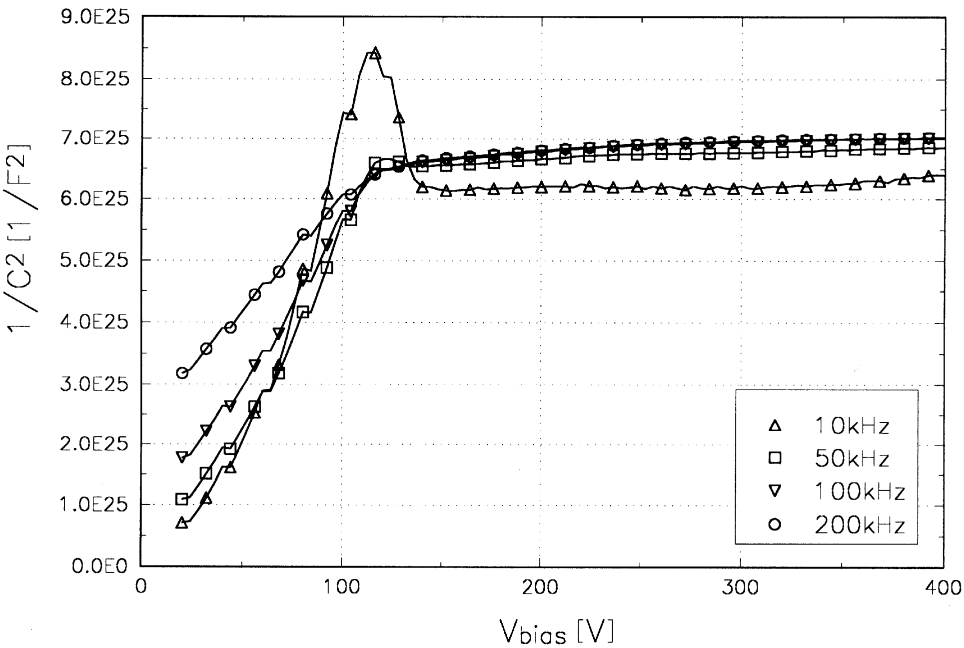

Fig. 9. $1/C^2_{back}$ versus bias voltage for strip number 60.

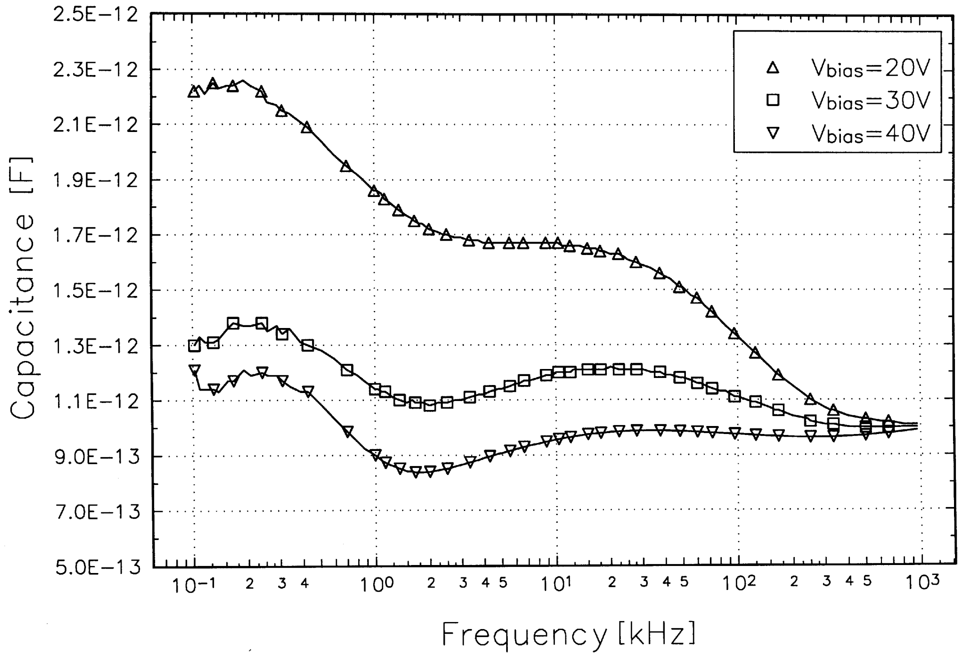

Fig. 10. C_{back} versus frequency for strip 115 at bias voltage below the full depletion.

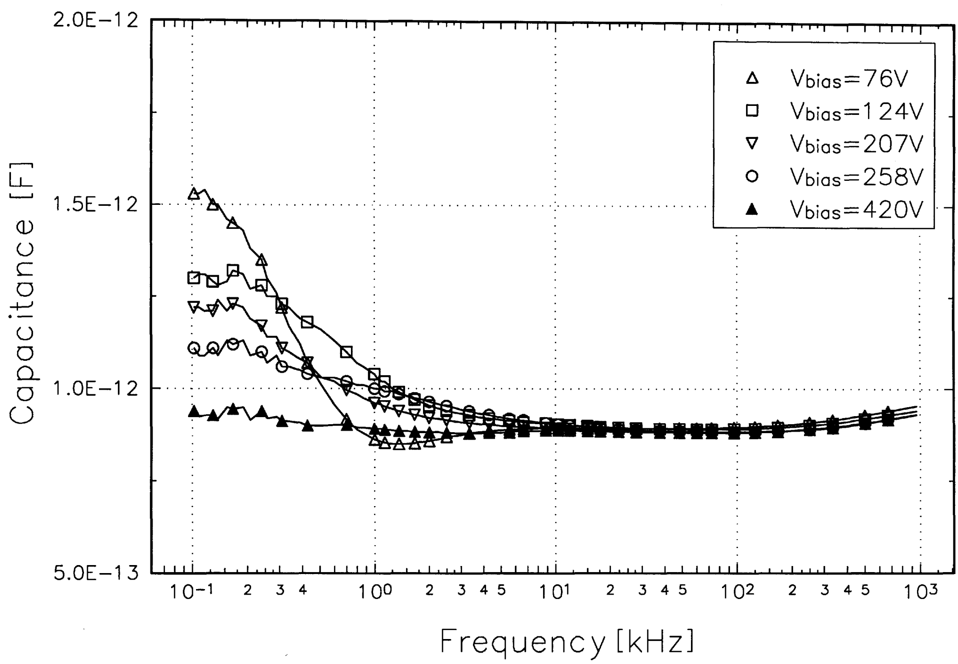

Fig. 11. C_{back} versus frequency for strip 115 at bias voltage above the full depletion.

3.2. Interstrip capacitance

Before irradiation no frequency dependence of the interstrip capacitance C_{int} was observed. In Fig. 12 typical curves of C_{int} versus bias voltage for inverted detectors are shown. All curves converge to the same, purely geometrical value for a very high bias voltage, which is about 10 times higher than the depletion voltage, similarly as it was for C_{back}. Measurements of C_{int} versus frequency for different bias voltages are shown in Fig. 13. Unless very high bias voltage is applied all curves show a similar behaviour with a smooth raise up to 5–50 kHz and then a very slow fall. The frequency dependence of C_{int} at voltages above the depletion voltage may result only from the electron surface layer in the interstrip region. In order to remove this layer and to recover the geometrical value of the capacitance a detector bias voltage much higher than the depletion voltage is required.

3.3. Interstrip resistance

In order to investigate the character of the interstrip region after type inversion, the interstrip I–V curves were measured. In Fig. 14 I–V curves measured with a floating detector backplane are presented. The non-linear shape of the curves shows clearly that the connection between the strips is not ohmic and indicates a structure consisting of two diodes, connected back to back. The DC interstrip resistance was evaluated from the I–V measurements for different bias voltages in the detector. As shown in Fig. 15, for low bias voltages the DC interstrip resistance increases slowly with increasing bias voltage and rapidly goes up when the bias approaches the depletion voltage. For the lowest bias voltages the minimum resistance was of the order of 1 MΩ. In Fig. 16 the AC interstrip resistance is shown as a function of bias voltage. For low frequencies (< 10 kHz) the AC resistance approaches the one obtained from the DC measurements. At higher frequencies it is lower but still high enough to assure good strip isolation, even before full depletion.

3.4. p + side after inversion

In order to investigate the region near the p + strips we measured the strip occupancy versus

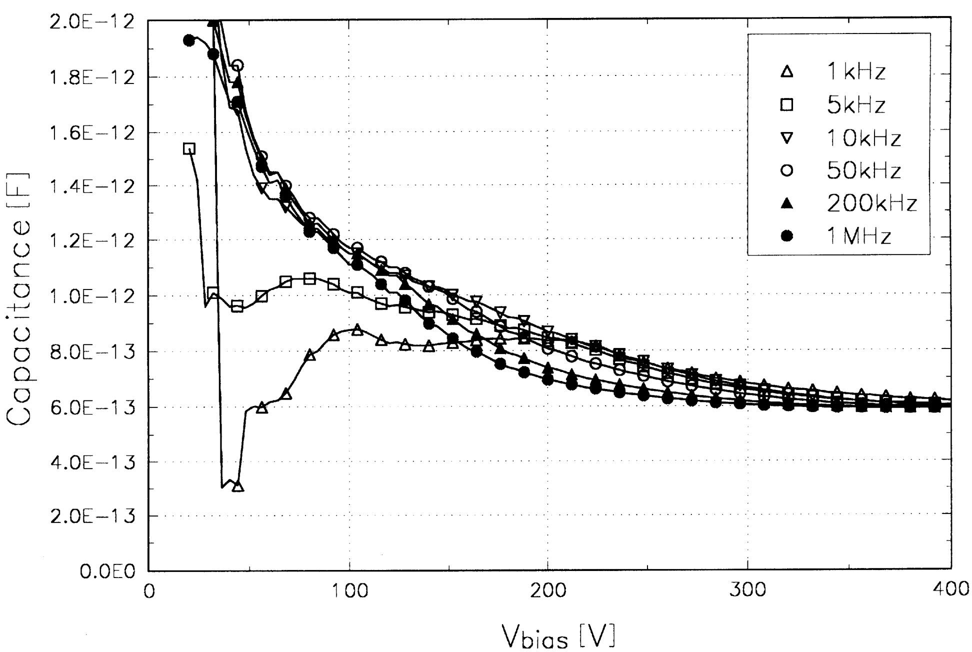

Fig. 12. C_{int} versus bias voltage for strip 115 with $V_{dep} = 40$ V.

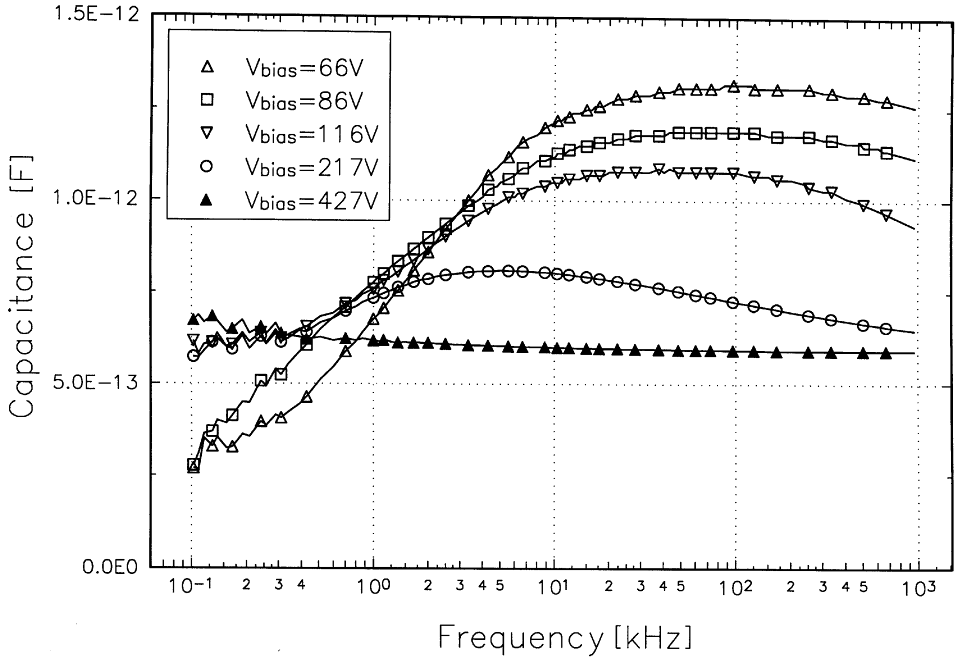

Fig. 13. C_{int} versus osc. frequency for strip 115 with $V_{\mathrm{dep}} = 40\,\mathrm{V}$.

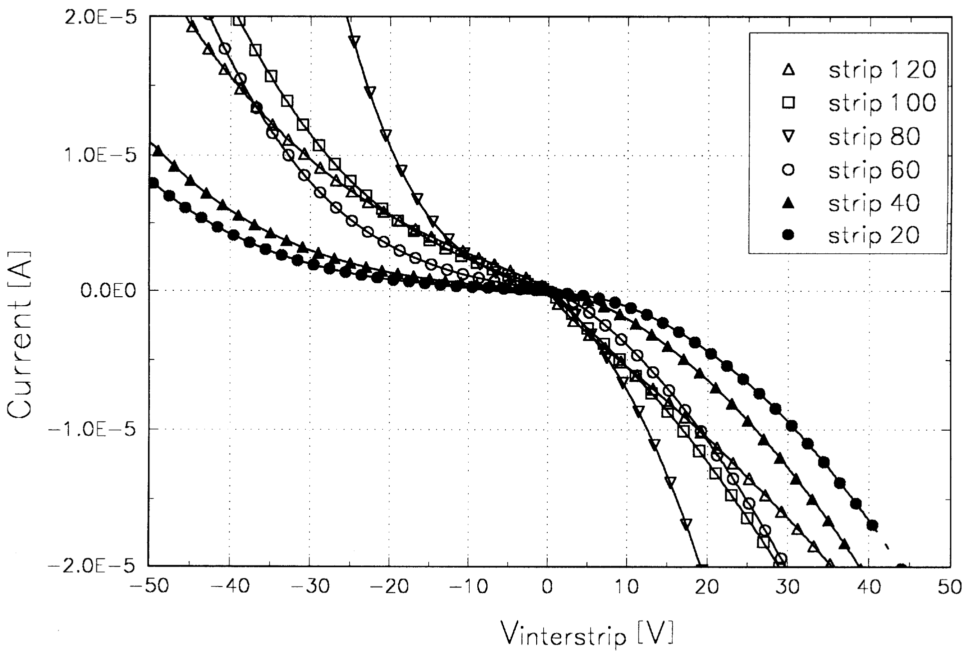

Fig. 14. Interstrip I–V curves for different strips measured at the floating detector backplane.

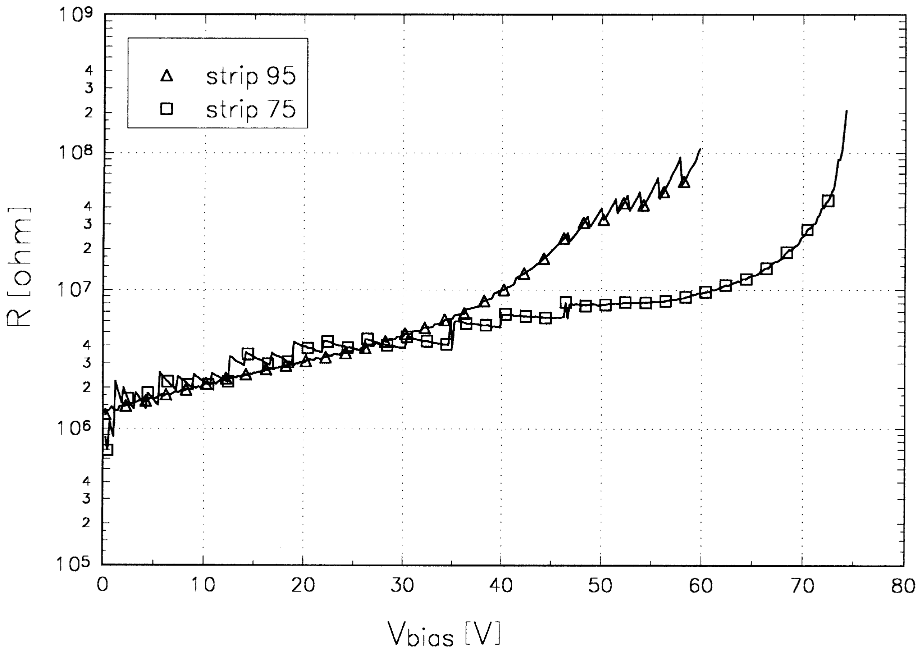

Fig. 15. Interstrip resistance obtained from I–V measurements.

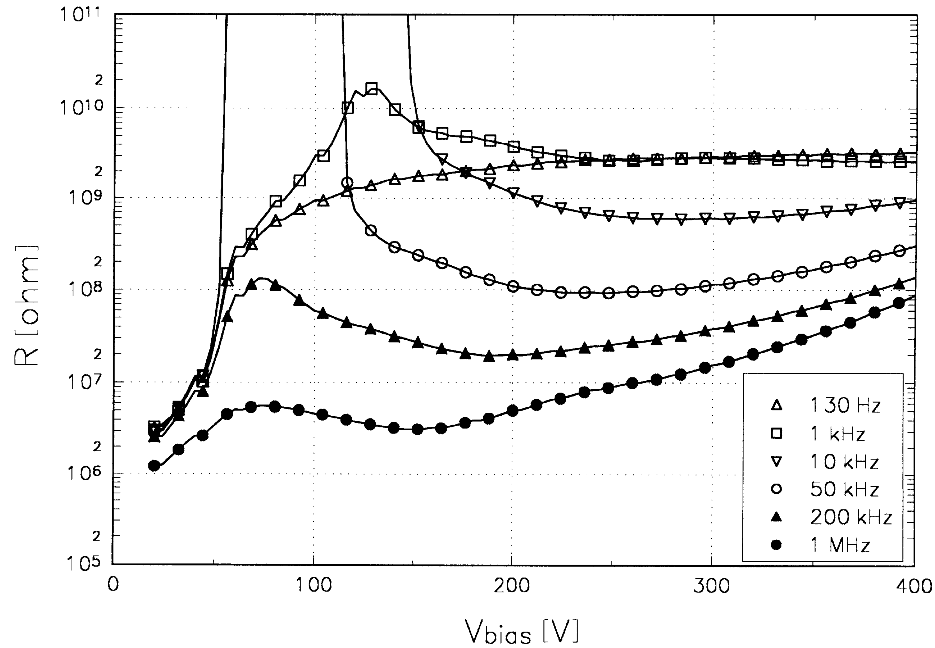

Fig. 16. Interstrip resistance obtained from AC measurements for strip 95.

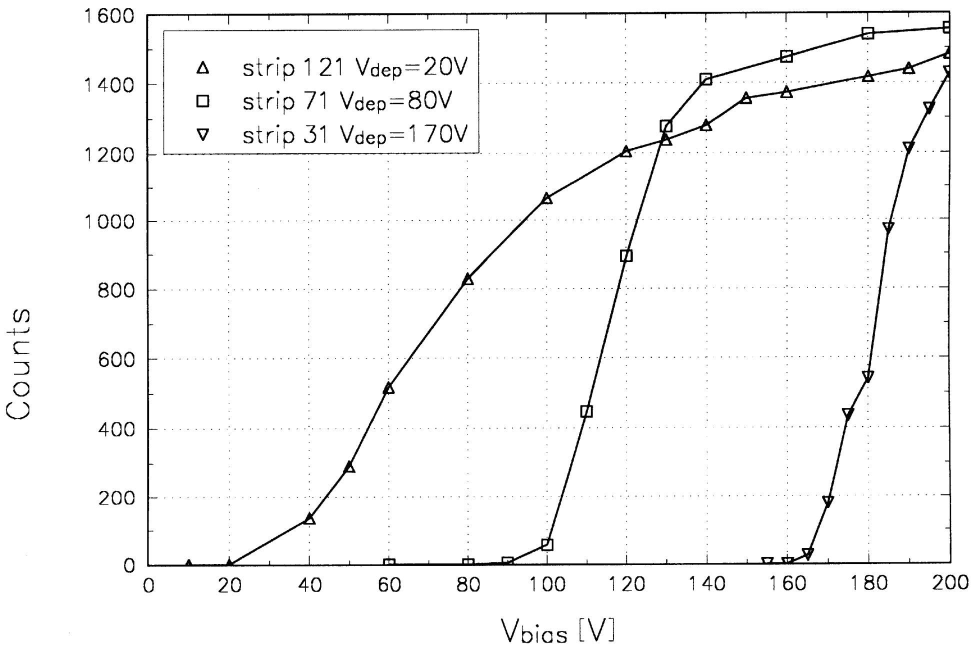

Fig. 17. Number of counts versus bias voltage obtained with infrared diode.

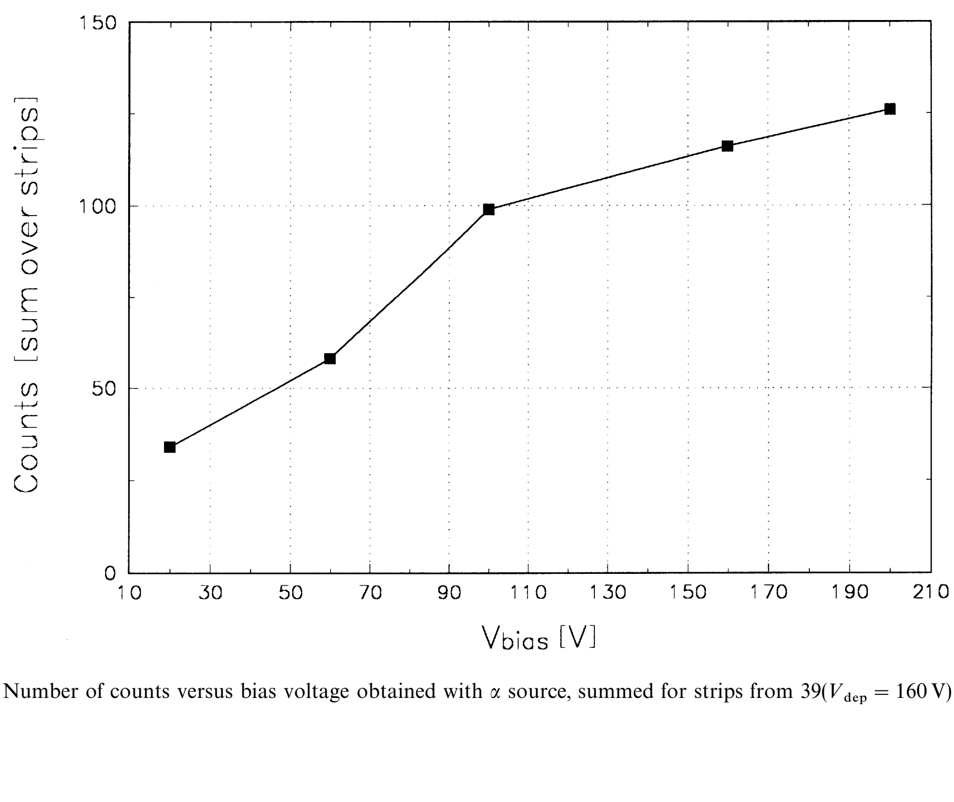

Fig. 18. Number of counts versus bias voltage obtained with α source, summed for strips from 39(V_{dep} = 160 V) to 64(V_{dep} = 100).

detector bias voltage, either exposing infrared diode light or α particles from an ^{241}Am source on the p+ side. In both cases the absorption length in silicon was of the order of 10 μm. For the americium source we set the threshold at ~2 MIP in order to reject the 60 keV X-rays. Because of the low intensity of the ^{241}Am source, we summed the number of counts over a group of strips. In Figs. 17 and 18 the number of counts versus bias voltage is shown for the infrared diode and for the ^{241}Am source, respectively. For the diode light there are no counts for bias voltages below the depletion voltage while for the α there are counts even for the lowest applied voltages, which are much lower than the depletion voltages for each strip in the group. The main difference between the α's and the diode light is the fact that light does not pass through the metal electrodes which cover and overlap the p+ implants. The comparison of the data from the diode light and the α's indicates that there is always a thin junction layer underneath the p+ implants. Results leading to the same conclusions were reported in Ref. [7].

4. Conclusions

The silicon strip detectors employed in the NA50 experiment provide us with an experimental evidence that standard p-on-n detectors work well after type inversion. There are three main factors supporting this conclusion, namely: a good detector efficiency is preserved, no detector breakdown is observed and there is a good isolation between p+ strips.

Concerning the physical behaviour of an individual detector we found that in order to remove the electron surface layer from the interstrip region and therefore to recover the purely geometrical values of detector capacitancies one needs to bias the detector with a voltage much higher than the depletion voltage. The measurements show that using a limited range of oscillator frequencies one can still use the C–V method to estimate the depletion voltage of inverted detectors. The performed measurements confirm the existence of a junction underneath the p+ implant. Still more work is needed to understand the physical origin of the observed frequency dependence of the radiation effects.

References

[1] B. Alessandro et al., Nucl. Instr. and Meth. A 409 (1998) 167.
[2] ATLAS Inner Tracker Technical Design Report, vol. 2, p. 394, CERN/LHCC/97-17.
[3] L. Dezille et al., Nucl. Instr. and Meth. A 386 (1997) 162.
[4] L. Andricek et al., ATLAS Internal Note INDET-NO-191, 10 November 1997.
[5] E. Fretwurst et al., Nucl. Instr. and Meth. A 342 (1994) 119.
[6] W. Dabrowski, K. Korbel, Nucl. Instr. Meth. A 276 (1989) 270.
[7] L.J. Beattie et al., ATLAS Internal Note INDET-NO-194, 9 December 1997.